Polymer Bulletin (2023) 80:11845–11859
https://doi.org/10.1007/s00289-022-04614-3

ORIGINAL PAPER

High-efficacy antimicrobial acyclic *N*-halamine-grafted polyvinyl alcohol film

Yuqing Shi[1] · Yijing He[1] · Jiarun Liu[1] · Xuan Tang[1] · Haidong Xu[1] · Jie Liang[1]

Received: 30 May 2022 / Revised: 8 November 2022 / Accepted: 20 November 2022 /
Published online: 6 December 2022

Abstract

With *N*,*N*′-methylenebisacrylamide (MBA) and polyvinyl alcohol (PVA) as raw materials, a polymer (PVA-MBA) containing *N*-halamine precursor functional groups was obtained via grafting reaction between the active hydroxyl groups on PVA and α, β-unsaturated functional groups of MBA under the catalysis of sodium carbonate in an aqueous solution. An acyclic *N*-halamine precursor-grafted PVA (MBA-PVA) film was formed by simply spreading PVA-MBA aqueous solution in a glass dish and drying it. An antimicrobial acyclic *N*-halamine-grafted PVA (PVA-MBA-Cl) film was achieved by spraying the diluted sodium hypochlorite solution onto the surface of PVA-MBA film. The performance test of PVA-MBA-Cl film under the optimal preparation conditions showed that the tensile performance and the hydrophobicity were improved, compared to the PVA film. The storage stability test indicated that the oxidative chlorine content Cl^+ (atoms/cm^2) of the as-prepared PVA-MBA-Cl film only reduced by 14.3% after storage for 9 weeks, showing that the antibacterial *N*-halamine functional groups in PVA-MBA-Cl film has excellent storage stability under room temperature. Antibacterial test showed that the PVA-MBA-Cl film had very strong antibacterial efficacies and could completely kill 1.28×10^6 CFU/mL *S. aureus* and 1.89×10^6 CFU/mL *E. coli* within 1 min. Therefore, PVA-MBA-Cl film will have more potential applications in food package.

Keywords Acyclic *N*-halamine · Antibacterial · Polyvinyl alcohol film · Food package

✉ Jie Liang
liangjie@shnu.edu.cn

[1] The Education Ministry Key Lab of Resource Chemistry and Shanghai Key Laboratory of Rare Earth Functional Materials, Shanghai Normal University, Shanghai 200234, People's Republic of China

Introduction

Microbial contamination and infection caused by pathogens are increasing global public health awareness. This issue is highlighted by the outbreak of Coronavirus disease (COVID-19) pandemic, which has caused more than 400 million confirmed cases and 6 million deaths worldwide. It is still increasing, causing immeasurable pain and economic losses [1]. The common way to prevent the proliferation of microorganisms and the spread of pathogens is disinfection and sterilization. It is well-known that the antibacterial agent is a core material, which can be divided into three categories: inorganic [2], organic [3–6], and natural antimicrobial agents [7, 8]. For the inorganic antibacterial agents, most of them are metal/metal oxide nanoparticles [9, 10], such as silver, copper, and zinc oxide. Their advantages are strong heat resistance, good antibacterial durability, and no drug resistance. However, complicated manufacturing processes, relatively expensive costs, and color issues restricted their applications. Commonly used organic antibacterial agents include aldehydes (ketones), phenols, quaternary ammonium salts [11], halides, thiophenes, biguanides, and diphenyl ethers. The advantages of organic antibacterial agents are wide range of sources, low production cost, fast sterilization rate, convenient processing, good stability, and their disadvantage is the poor heat resistance. The natural antibacterial agents such as chitosan, bacteriocin, lysozyme, plant essential oils are mainly obtained from animal or plant extracts or synthesized by microorganisms. The advantages of them are high safety, non-toxicity, good biocompatibility, and abundant resources. Their disadvantages are poor heat resistance, short pot life, and restricted production condition and equipment. As a kind of organic antibacterial agents, *N*-halamine antibacterial agents have higher stability, much stronger antibacterial efficacies, less harm to the environment, and easier use for antibacterial treatment on the surface of materials. It is generally believed that the sterilization mechanism of *N*-halamine antibacterial agents is that *N*-halamine molecules first contact the bacteria, and then the oxidized chlorines oxidize the receptors in the cell, thereby destroying the bacterial metabolism and killing them. At the same time, the bactericidal ability of *N*-halamines can be regenerated after rinsing with dilute bleaching water solution to convert the N–H bonds in the molecules into N–Cl ones [6, 12, 13].The immobilization of the antibacterial agent refers to the process of introducing the antibacterial groups to the surface of the material by physical action [14–18], such as van der Waals force or electrostatic attraction and covalent bond coupling. At present, the immobilization methods of *N*-halamine antibacterial agents mainly include physical modification methods represented by surface coating and blending, and chemical modification methods [18, 19] represented by surface electrophilic, nucleophilic reactions, and surface graft polymerization reactions [20–24]. When the material is modified by physical coating, the interaction force between the antibacterial agent molecules and the material is weak, the antibacterial agent molecules are easy to detach during use. When the material is modified by physical blending, most of the antibacterial agent molecules are deeply buried inside the material and are difficult to exert antibacterial

effect, resulting in a relatively low utilization rate of antibacterial agents. In this paper, the chemical grafting method [25–28] was used to obtain modified film [29–31] materials with the superior stability of antimicrobial *N*-halamine groups and high-efficacy antimicrobial capacity.

Environmental pollution caused by plastic waste is an increasingly serious global problem. Many industries are turning the way of packaging food to a more sustainable choice and developing biodegradable antibacterial food packaging materials. In the meantime, Omicron variant (COVID-19) pandemic broke out in Shanghai. There are still many positive cases during long-term home closure. Experts say there is a risk of Omicron carrying in group buying packages and items. As a result, the development of antibacterial films for packaging applications is a meaningful research field. PVA is a water-soluble polymer material, which has the features of degradability, biocompatibility, non-toxicity, safety, and environmental friendliness. It has broad application prospects in respect of packaging materials. Li et al. [32] prepared a cyclic *N*-halamine-grafted PVA film and evaluated its antimicrobial efficacy against *Escherichia coli* O157:H7 and *Staphylococcus aureus* within contact times of 5 and 10 min. However, the storage of antimicrobial *N*-halamine groups in the PVA film was not unsatisfactory. In this paper, we developed a three-step process to prepare an acyclic *N*-halamine-grafted antibacterial PVA (PVA-MBA-Cl) film. The preparation route of antimicrobial PVA-MBA-Cl film and its

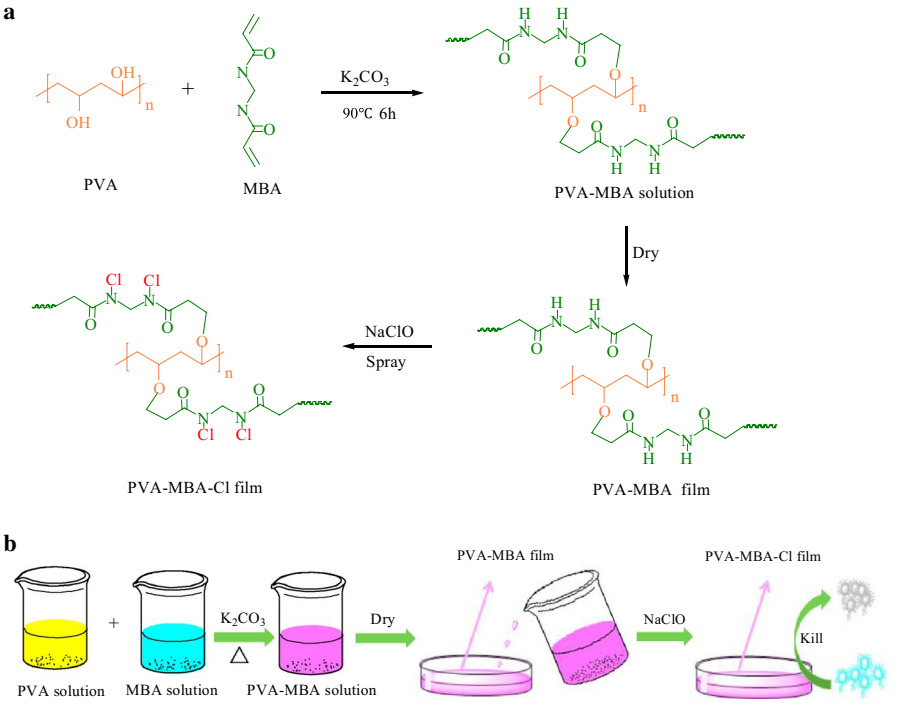

Fig. 1 Synthetic route for antimicrobial PVA-MBA-Cl film (**a**) and its schematic diagram of the preparation and sterilization (**b**)

schematic diagram of the preparation and sterilization are shown in Fig. 1. The two terminals of MBA molecules are the carbon–carbon double bonds, which obviously could react with the hydroxy groups of PVA in water under the base catalysis to form a MBA-grafted PVA (PVA-MBA) aqueous solution. After PVA-MBA film was formed, the antimicrobial function was achieved via converting the amide groups of MBA to *N*-halamine groups with an addition of NaClO aqueous solution. The as-prepared PVA-MBA-Cl film exhibits super antibacterial efficacies and excellent stability of antimicrobial *N*-halamine groups.

Experimental section

Materials and instruments

Methylene-bis-acrylamide (MBA) and polyvinyl alcohol (PVA, the average molar mass is 7.5×10^4 g/mole) were purchased from Macleans Shanghai Reagent Co., Ltd. Sodium hypochlorite, sulfuric acid, sodium carbonate, and potassium iodide were bought from Sinopharm Chemical Reagent Co., Ltd. *Staphylococcus aureus* (*S. aureus*) and *Escherichia coli* (*E. coli*) were provided by Shanghai Institute of Materia Medica, Chinese Academy of Sciences.

Hitachi S4800 scanning electron microscope was used to obtain field emission scanning electron microscope (FE-SEM) images. X-ray photoelectron spectroscopy (XPS) spectra were obtained by using PerkinElmer PHI 5000 ESCT System. Dmax-2000 x-ray diffraction was used to obtain x-ray diffraction (XRD) spectra. Thermo Scientific NicoletiN10 infrared spectrometer was adopted to obtain Fourier-transform infrared spectroscopy (FT-IR) spectra. JC2000D2 contact angle measuring instrument bought from Shanghai Zhongchen Digital Technology Co., Ltd. was used to characterize by the contact angle.

Preparation of PVA-MBA film

PVA (4.40 g) was dissolved in 80 mL of distilled water and stirred. The temperature was gradually risen to 90 °C and was kept at 90 °C for about 30 min to ensure that PVA was dissolved completely. MBA (0.088 g) and K_2CO_3 (0.300 g) were dissolved in 20 mL of distilled water and stirred. After the MBA and K_2CO_3 solution was added into PVA solution. The reaction mixture solution was stirred for 6 h at 90 °C to form a PVA-MBA aqueous solution. PVA-MBA aqueous solution was spread on a glass dish and air-dried to form a PVA-MBA film.

Preparation of PVA-MBA-Cl film

20 mL of 5.0% sodium hypochlorite solution was added into 100 mL distilled water at room temperature. The pH of the solution was adjusted to about 7 via slowly adding sulfuric acid solution. Then, the diluted sodium hypochlorite solution was

sprayed onto the surface of PVA-MBA film. After 2 h, the film was washed with distilled water to ensure no free sodium hypochlorite on the surface of the film.

Determination of oxidative chlorine content of PVA-MBA-Cl film

Iodometric method was used to determine the oxidative chlorine content of PVA-MBA-Cl film. The specific process was as follows: about 1 cm × 1 cm of PVA-MBA-Cl film was added into 45 mL of 0.1 N H_2SO_4 solution, and then about 0.15 g potassium iodide was added to the above solution. The above solution was titrated with 0.0100 N sodium thiosulfate standard solution until the color of the titrated solution became light yellow. After 0.30 mL of 1% starch aqueous solution was added, the solution was continued to be titrated with sodium thiosulfate standard solution to reach the end of titration when the titrated solution became colorless. The oxidative chlorine content of PVA-MBA-Cl film can be calculated by the following formula:

$$\mathrm{Cl}^{+}\left(\mathrm{atoms/cm}^{2}\right)=\frac{N\times V\times 6.02\times 10^{23}}{2\times S}$$

where Cl^+ (atoms/cm^2) is the oxidation state chlorine content on the surface of the film, N is the molar concentration of the sodium thiosulfate standard solution, V is the volume (L) of the sodium thiosulfate standard solution consumed, S is the surface area of PVA-MBA-Cl film (cm^2).

Tensile strength [33, 34] and elongation at break of PVA-MBA-Cl film

Take PVA, PVA-MBA, PVA-MBA-Cl films and cut them into the intact 10 cm × 1 cm films. Make 3 samples of each film and fix the film on the texture analyzer. The film was made up to a distance of 3 cm, the stretching speed was 2 cm/min, and the test results were averaged. The thickness of the PVA-MBA-Cl film was measured with a micrometer, and 10 points were taken at different places of the film, and the average value was taken as the thickness of the film. Regarding the tensile strength δ, the formula is as follows:

$$\delta=\frac{F}{\mathrm{bd}}$$

where δ is the tensile strength (MPa) of the film, F is the maximum force (N) during the entire stretching process, b is the width (mm) of the film, and d is the thickness (mm) of the film.

Contact angle test

The hydrophilicity change of the film was determined by measuring the contact angle of the film. The specific steps are as follows:

The ultrapure water droplets were tested on the surface of the film for 5 s. The test temperature was room temperature and the volume was fixed by the device needle. Each sample was measured in turn and the test was averaged three times.

Solubility test

The PVA film, PVA-MBA film, and PVA-MBA-Cl film were cut into a size of 1 cm × 1 cm and dried for 12 h in a vacuum oven at 45 ℃.The PVA film, PVA-MBA film, and PVA-MBA-Cl film were respectively placed in a desiccator and cooled to room temperature and weighed as an initial mass of m_0.The PVA film, PVA-MBA film, and PVA-MBA-Cl film were completely immersed in a beaker containing 45 mL of deionized water for 24 h before being taken out. The water on the surface of the film was wiped dry and dried for 12 h in a vacuum oven at 45 °C. Weigh the film, the mass after dissolution (m_1), the dissolution rate is calculated as follows:

$$D = \frac{m_0 - m_1}{m_0} \times 100\%$$

where D is the solubility (%), m_0 (g) is the initial mass, m_1 (g) is the mass after dissolution.

Water absorption test

The PVA film, PVA-MBA film, and PVA-MBA-Cl film were cut into a size of 1 cm × 1 cm and then dried in a vacuum oven at 45 ℃ for 12 h. The film was taken out and placed in a desiccator to cool to room temperature. The mass of the film was weighed and recorded as the initial mass m_0. The film was placed flat into a small amount of deionized water in a watch glass and sealed with plastic wrap for 24 h. Take out the sample and weigh it as the final film mass m_1. The water absorption formula is as follows:

$$C = \frac{m_1 - m_0}{m_0} \times 100\%$$

where C is the water absorption (%), m_0 (g) is the initial mass, and m_1 (g) is the mass after water absorption.

Storage stability test of *N*-halamine functional groups in PVA-MBA-Cl film

The stability of the *N*-halamine functional groups in PVA-MBA-Cl film was determined by measuring the change of the oxidized chlorine content in PVA-MBA-Cl film during the storage. The film was stored at room temperature in a dark condition, and one portion was taken every seven days for measurement of the Cl^+ content. Specific steps are as follows: the as-prepared PVA-MBA-Cl film was cut into a size of 1 cm × 1 cm. The Cl^+ content of the film was determined for three times after

each week to explore the change tendency of the Cl^+ content of PVA-MBA-Cl film during storage.

Antibacterial performance test of PVA-MBA-Cl film [35]

In this paper, Gram-positive bacterium *S. aureus* and Gram-negative bacterium *E. coli* were selected to measure the antibacterial efficacy of the PVA-MBA-Cl film. The process is as follows: Firstly, 25 μL of the buffered bacterial solution (pH was about 7) was added onto the surface of the film with a size of 2 cm × 2 cm and then the other film with the same size was covered on it. Above these two films, a sterile weight was pressed onto them. After contact time of 1 min, 5 min, 10 min, and 30 min, the square films were transferred into 10.0 mL of 0.02 N sterile sodium thiosulfate solution in a sterile centrifuge tube to remove oxidative chlorines, and vortexed for 2 min. Secondly, after vortexed, the above solution was serially diluted with sterile phosphate buffer solution (pH was about 7). Finally, 100 μL of the diluted solution was taken in a solid medium, and the number of colonies on the plate medium was counted after incubation at 37 °C for 24 h.

Results and discussion

Preparation of PVA-MBA-Cl film

Synthesis of antibacterial films for packaging applications is significant fields of research [36]. In this paper, we developed a simple and green process to prepare a very high-efficacy antimicrobial film, an acyclic *N*-halamine-modified PVA (PVA-MBA-Cl) film. Firstly, an aqueous solution of *N*-halamine precursor-grafted PVA (PVA-MBA solution) was prepared via the oxa-Michael addition reaction between the active hydroxyl groups on PVA and α,β-unsaturated functional groups of MBA under the catalysis of sodium carbonate in an aqueous solution. Secondly, PVA-MBA film was formed by spreading a certain amount of PVA-MBA solution on a glass dish and drying it. Finally, after spraying the diluted sodium hypochlorite solution on the surface of PVA-MBA film, PVA-MBA-Cl film was formed. Higher oxidative chlorine content on the surface of the film means more *N*-halamine functional groups on the film surface and stronger antimicrobial efficacy. It is our desire to obtain a PVA-MBA-Cl film with higher oxidative chlorine content to ensure stronger and lasting antibacterial efficacy without affecting other important properties of the film such as the transparency and tensile strength. For this purpose, we studied the effects of mass ratio of MBA and PVA (m_{MBA}/m_{PVA}), mass of catalyst, reaction time, reaction temperature, and chlorination time on the oxidative chlorine content on the surface of the as-prepared PVA-MBA-Cl film.

Figure 2 showed the effects of m_{MBA}/m_{PVA}, mass of catalyst, reaction temperature reaction time, and chlorination time on the oxidative chlorine content on the surface of the as-prepared PVA-MBA-Cl film. As seen in Fig. 2a, it was found that the oxidative chlorine content increased from 1.46×10^{19} to 6.86×10^{19} atoms/cm^2 with an increase of m_{MBA}/m_{PVA} from 1:200 to 12:200 in the aqueous solution. The

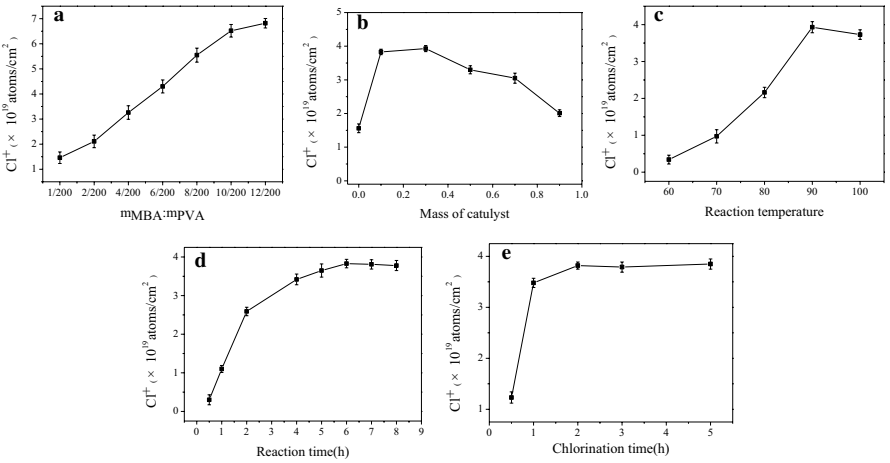

Fig. 2 Effects of m_{MBA}/m_{PVA} (**a**), mass of catalyst, reaction temperature (**c**), reaction time (**d**), and chlorination time (**e**) on the oxidative chlorine content (atoms/cm^2) of the as-prepared PVA-MBA-Cl film [m_{MBA}/m_{PVA} = 4:200 (**b**–**e**); mass of catalyst = 0.30 g (**a**, **c**– **e**); reaction temperature: 90 ℃ (**a**, **b**, **d**, **e**); reaction time: 6 h (**a**–**c**, **e**); chlorination time: 2 h (**a**–**d**)]

increase in the oxidative chlorine content is attributed to more MBA grafted onto PVA with the increase of m_{MBA}/m_{PVA}. However, while m_{MBA}/m_{PVA} was 6:200, some white substance could be seen in the film, which affected the transparency of the film. Therefore, 4:200 should be an appropriate m_{MBA}/m_{PVA} for the preparation of PVA-MBA-Cl film. As shown in Fig. 2b, as the mass of catalyst increased from 0 to 0.30 g, the oxidative chlorine content increased from 1.56×10^{19} to 3.83×10^{19} atoms/cm^2. This is because the addition of K_2CO_3 can speed up the oxa-Michael addition reaction, which makes more MBA grafted on the PVA. However, when the mass of K_2CO_3 was more than 0.30 g, the increase in catalyst mass resulted in the decrease in the oxidative chlorine content. This is mainly because that much more K_2CO_3 in the aqueous solution may accelerate the amide hydrolysis of MBA. Therefore, 0.30 g should be an appropriate mass of catalyst for the preparation of PVA-MBA-Cl film. As shown in Fig. 2c, the oxidative chlorine content increased from 0.34×10^{19} to 3.81×10^{19} atoms/cm^2 with the increase in reaction temperature from 60 °C to 90 °C. When the reaction was at 100 °C, the oxidative chlorine content decreased, compared to that at 90 °C. Therefore, 90 °C should be an appropriate reaction temperature for the preparation of PVA-MBA-Cl film. As shown in Fig. 2d, the oxidative chlorine content increased from 1.10×10^{19} to 3.81×10^{19} atoms/cm^2 with the increase in reaction time from 1 to 6 h. After 6 h, continuous increasing the reaction time from 6 to 8 h, the oxidative chlorine content remained almost unchanged. Therefore, 6 h should be an appropriate reaction time for the preparation of PVA-MBA-Cl film. As shown in Fig. 2e, the oxidative chlorine content increased from 1.10×10^{19} to 3.81×10^{19} atoms/cm^2 with the increase in chlorination time from 0.5 h to 2 h. After 2 h, continuously increasing the chlorination time from 2 to 5 h, the oxidative chlorine content didn't change a lot. Therefore, 2 h should be an appropriate chlorination time for the preparation of PVA-MBA-Cl film.

Characterization of PVA-MBA-Cl film

FE-SEM

The morphology of film surfaces was inspected by FE-SEM. Figure 3 showed FE-SEM images of the surface of PVA(a), PVA-MBA(b) and PVA-MBA-Cl(c), the section of PVA(d), PVA-MBA(e) and PVA-MBA-Cl(f) films. It is obvious that the surface of the films are all flat. In general, the grafting and chlorination did not rupture and damage the surface of the film. However, the sectional structures of PVA-MBA film and PVA-MBA-Cl film are more complicated than that of PVA film. The possible reason is that the grafting reaction caused the molecular cross-linking in the modified film.

FT-IR and XPS spectra

The FT-IR spectra of PVA and PVA-MBA-Cl films are shown in Fig. 4a. It could be seen that the strong –OH stretching vibration absorption peaks appear close to 3330 cm^{-1} for two spectral lines, declaring that the functional group –OH does exist in two films. The peak area of PVA-MBA-Cl film is significantly smaller, compared with that of PVA film, indicating that the part of the –OH on the PVA molecular chain reacts with the MBA, thereby reducing the amount of –OH on the PVA-MBA-Cl molecular chain [37]. The peak at 2924 cm^{-1} is ascribed to the C-H stretching vibration in the polyvinyl alcohol unit for both two samples. Compared with PVA, PVA-MBA-Cl film exhibits a new peak at 2849 cm^{-1}, which corresponds to the symmetrical stretching vibration of the C–H on CH_2–CH_2–. Because the double bond on the MBA molecule is opened to become a continuous CH_2–CH_2– functional group while PVA react with MBA. PVA-MBA-Cl film has a new peak at 826 cm^{-1}, which

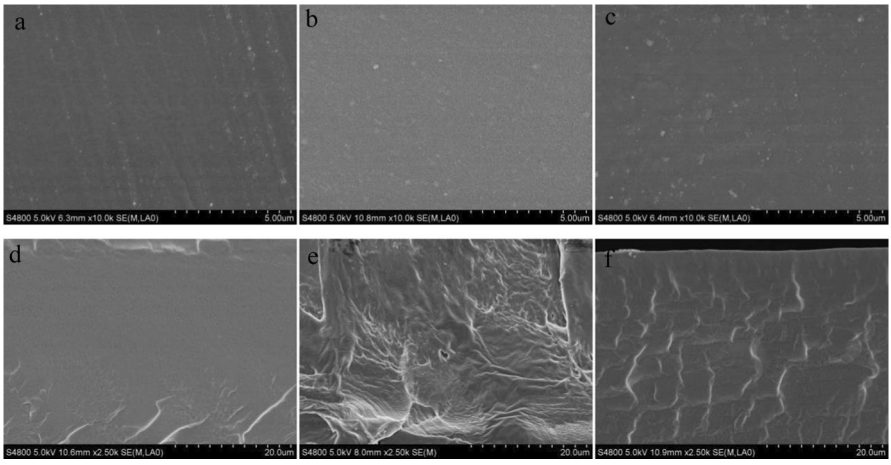

Fig. 3 FE-SEM images of the surface of PVA (**a**), PVA-MBA (**b**) and PVA-MBA-Cl (**c**), the section of PVA (**d**), PVA-MBA (**e**) and PVA-MBA-Cl (**f**) films

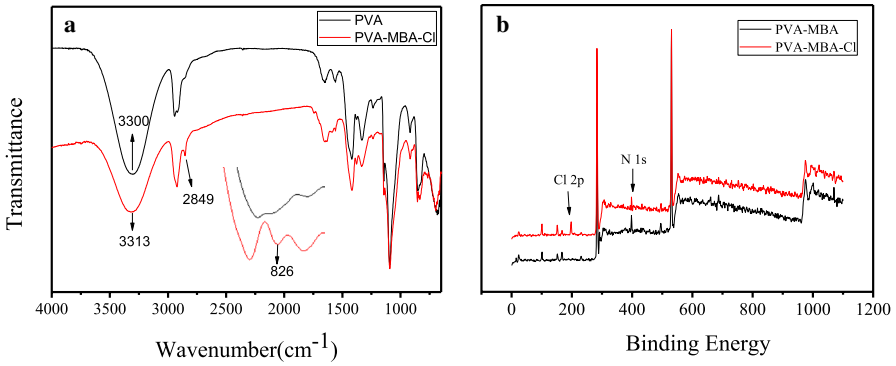

Fig. 4 FT-IR (**a**) and XPS (**b**) spectra of PVA and PVA-MBA-Cl films

corresponds to the stretching vibration of the N–Cl bond. This is caused by the conversion of N–H bonds on the amide groups of MBA into N-Cl ones after chlorination [38], indicating that MBA molecules have been successfully grafted onto PVA and the amide groups of MBA have been chlorinated. The XPS spectra of PVA-MBA and PVA-MBA-Cl films are shown in Fig. 4b. As seen in Fig. 4b, compared to PVA film, PVA-MBA-Cl film has a new Cl 2p peak at 200 eV [39, 40], indicating that the chlorination reaction has been successfully carried out.

Performance evaluation

Water absorption, solubility, tensile strength, and elongation at break

Figure 5a showed the water absorption and the solubility of PVA, PVA-MBA, and PVA-MBA-Cl films. It is obvious that PVA-MBA film has lower water absorption and solubility than PVA film, which is due to the nucleophilic reaction between the –OH in PVA and MBA under the action of a base to reduce the hydrophilic groups in the molecules. Compared to PVA-MBA film, PVA-MBA-Cl film exhibits higher

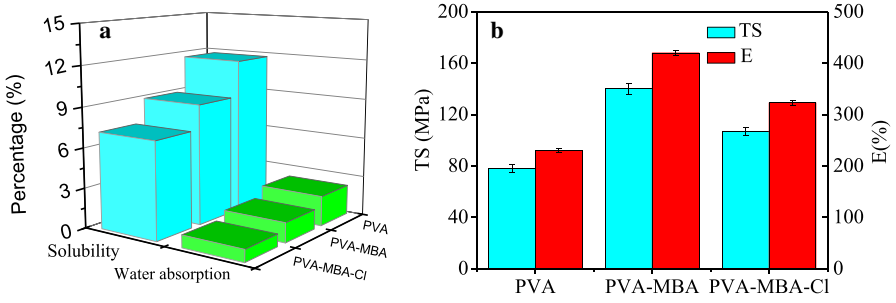

Fig. 5 Water absorption, solubility, tensile strength, and elongation at break of PVA, PVA-MBA and PVA-MBA-Cl films

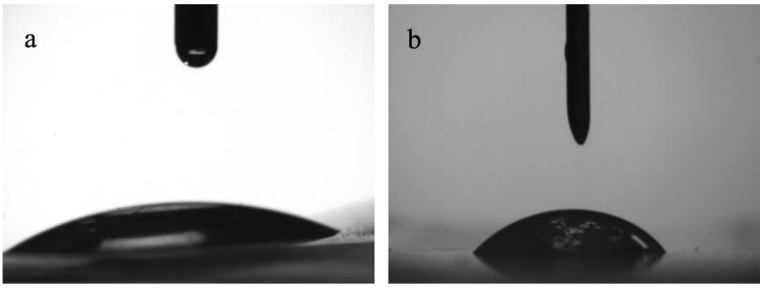

Fig. 6 Contact angles (**a**) of PVA and PVA-MBA-Cl (**b**) films

Table 1 Contact angles of PVA and PVA-MBA-Cl films

Sample	PVA film	PVA-MBA-Cl film
Contact angle/°	37	49

water absorption and solubility due to the destruction of the intermolecular action [36]. The tensile strengths and elongations at break of PVA, PVA-MBA, and PVA-MBA-Cl films are shown in Fig. 5b. Compared to PVA film, PVA-MBA film exhibits much higher tensile strength and elongation at break. The improvement in tensile strength and elongation at break is ascribed to the cross-linking reaction between PVA and MBA. Very interestingly, PVA-MBA-Cl film has lower tensile strength, but much higher elongation than PVA film. The decrease in tensile strength is due to the depolymerization of the PVA molecules. The increase in elongation is ascribed to crystallinity decrease in PVA molecular chain due to the oxidative NaClO [41].

Contact angle

Figure 6 showed the contact angles of PVA and PVA-MBA-Cl films and the data of the contact angles are summarized in Table 1. Compared to PVA film, PVA-MBA-Cl film exhibits much larger contact angle. The improvement in contact angle is ascribed to the cross-linking reaction between PVA and MBA. MBA consumes the part of polar –OH groups on the PVA molecular chain. Therefore, the hydrophilicity of the film is weakened, resulting in a larger contact angle. It is very interesting that the grafted MBA improves the hydrophobicity of the modified PVA film and solves the problem that the PVA film is too hydrophilic and easily soluble.

Storage stability of *N*-halamine functional groups in PVA-MBA-Cl film

Figure 7 showed the storage stability of the antibacterial *N*-halamine functional groups in PVA-MBA-Cl film. It was found that the oxidative chlorine content of PVA-MBA-Cl film decreased by 14.3% after stored for 9 weeks. It means that the antibacterial *N*-halamine functional groups in PVA-MBA-Cl film have excellent

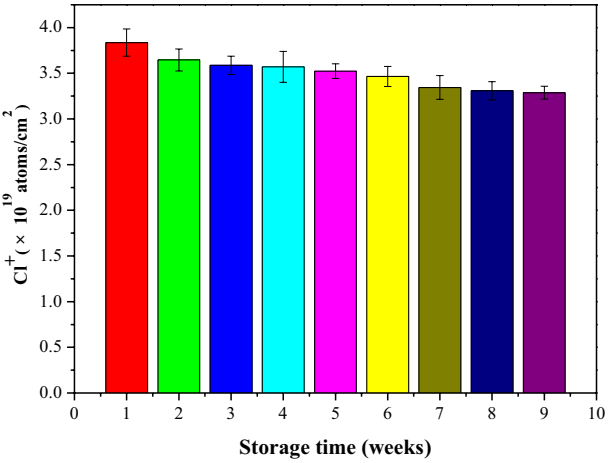

Fig. 7 The storage stability of the antibacterial *N*-halamine functional groups in the PVA-MBA-Cl film

storage stability under room temperature. Therefore, the as-prepared PVA-MBA-Cl film has long-lasting antibacterial effect.

Antibacterial performance

S. aureus and *E. coli* were adopted for the antibacterial efficacy test of PVA, PVA-MBA, and PVA-MBA-Cl films. The results are summarized in Table 2. It was found that PVA-MBA-Cl film exhibited very strong antibacterial efficiencies against both *S. aureus* and *E. coli*. PVA-MBA-Cl film with an oxidative chlorine content of 3.82×10^{19} atoms/cm^2 could completely inactivate 1.28×10^6 CFU/mL *S.aureus* and 1.89×10^6 CFU/mL *E. col*i within a contact time of 5 min. By comparison, the unchlorinated PVA and PVA-MBA films had low reduction of bacteria. They

Table 2 Antibacterial efficiencies of PVA, PVA-MBA, and PVA-MBA-Cl films against bacteria *S. aureus* and *E. coli*

Sample	Contact time (min)	Antibacterial rate (%)	
PVA		*S. aureus*[a] reduction (%)	*E. coli*[b] reduction (%)
PVA-MBA	30	9.71	12.69
	30	16.45	20.21
	1	99.99	99.99
PVA-MBA-Cl	5	100	100
	10	100	100
	30	100	100

[a]Inoculum population: 1.28×10^6 CFU/mL

[b]Inoculum population: 1.89×10^6 CFU/mL

respectively provided 9.71% and 16.45% reductions of *S. aureus* and 12.69% and 20.21% reductions of *E. coli* within a contact time of 30 min. In comparison with some *N*-halamine coatings reported from Worley's group, the as-prepared PVA-MBA-Cl film shows stronger antimicrobial efficacies [42, 43].

Conclusion

In summary, an environmentally friendly method was developed to prepare a high-efficacy antibacterial acyclic *N*-halamine-grafted PVA (PVA-MBA-Cl) film. The whole process only used water as the solvent. Definitely, the as-prepared PVA-MBA-Cl film exhibited very strong antibacterial efficacies and excellent storage stability of antimicrobial *N*-halamine moieties. Very interestingly, the as-prepared PVA-MBA-Cl film also showed lower water absorption and solubility, higher tensile strength and elongation at break than PVA film. With all above-mentioned advantages, it is very clear that the antimicrobial PVA-MBA-Cl film will have potential applications in food packaging. Moreover, the successful development of a practical process to prepare an antibacterial *N*-halamine precursor solution provides more possibilities for the development of useful antibacterial coating materials for various applications such as bactericidal paintings and long-lasting disinfection of hard surface in future.

Acknowledgements The authors acknowledge the financial support from Shanghai Pujiang Talent Project (11PJ1407600) for this work. They also acknowledge experimental support from the Program of Shanghai Normal University (DZL124) PCSIRT (RT1269).

References

1. Parihar A, Sonia ZF, Akter F et al (2022) Phytochemicals-based targeting RdRp and main protease of SARS-CoV-2 using docking and steered molecular dynamic simulation: a promising therapeutic approach for tackling COVID-19. Comput Biol Med 154:105468
2. Ji J, Zhang W (2009) Bacterial behaviors on polymer surfaces with organic and inorganic antimicrobial compounds. J Biomed Mater Res Part A 88(2):448–453
3. Shen M, Liao X, Xianyu Y et al (2022) Polydimethylsiloxane membranes incorporating metal–organic frameworks for the sustained release of antibacterial agents[J]. ACS Appl Mater Interfaces 14(10):12662–12673
4. Taghipour T, Karimipour G, Ghaedi M et al (2018) Mild synthesis of a Zn (II) metal organic polymer and its hybrid with activated carbon: application as antibacterial agent and in water treatment by using sonochemistry: optimization, kinetic and isotherm study[J]. Ultrason Sonochem 41:389–396
5. Sun Y, Sun G (2002) Synthesis, characterization, and antibacterial activities of novel *N*-halamine polymer beads prepared by suspension copolymerization. Macromolecules 35(23):8909–8912
6. Dong A, Sun Y, Lan S et al (2013) Barbituric acid-based magnetic *N*-halamine nanoparticles as recyclable antibacterial agents. ACS Appl Mater Interfaces 5(16):8125–8133
7. Gould GW (1996) Industry perspectives on the use of natural antimicrobials and inhibitors for food applications. J Food Prot 59(13):82
8. Tiwari Brijesh K, Valdramidis Vasilis P, O'Donnell Colm P, Kasiviswanathan M, Paula B, Cullen PJ (2009) Application of natural antimicrobials for food preservation. J Agric Food Chem 57(14):5987
9. Hernández-Sierra JF, Ruiz F, Pena DCC et al (2008) The antimicrobial sensitivity of Streptococcus mutans to nanoparticles of silver, zinc oxide, and gold. Nanomed Nanotechnol Biol Med 4(3):237–240

10. Nan G, Yingjie C, Jiang J (2013) Ag@Fe2O3-GO nanocomposites prepared by a phase transfer method with long-term antibacterial property. ACS Appl Mater Interfaces 5(21):11307
11. Chen Y, Chen Q, Wang Z et al (2022) Bactericidal silicone with one quaternary ammonium salt and two *N*-halamine sites in the repeating unit for improved biocidability on magnetic submicrospheres. J Mater Sci 57:1–15
12. Natan M, Gutman O, Lavi R et al (2015) Killing mechanism of stable *N*-halamine cross-linked polymethacrylamide nanoparticles that selectively target bacteria. ACS Nano 9(2):1175–1188
13. Xu J, Wang Z, Yu L et al (2013) A novel reverse osmosis membrane with regenerable anti-biofouling and chlorine resistant properties. J Membr Sci 435:80–91
14. Cloutier M, Mantovani D, Rosei F (2015) Antibacterial coatings: challenges, perspectives, and opportunities. Trends Biotechnol 33(11):637–652
15. Zhou B, Li Y, Deng H et al (2014) Antibacterial multilayer films fabricated by layer-by-layer immobilizing lysozyme and gold nanoparticles on nanofibers. Colloids Surf B 116:432–438
16. Imazato S, Ehara A, Torii M et al (1998) Antibacterial activity of dentine primer containing MDPB after curing. J Dent 26(3):267–271
17. Wang Q, Fan X, Hu Y et al (2009) Antibacterial functionalization of wool fabric via immobilizing lysozymes. Bioprocess Biosyst Eng 32(5):633–639
18. Huh MW, Kang IK, Lee DH et al (2001) Surface characterization and antibacterial activity of chitosan-grafted poly (ethylene terephthalate) prepared by plasma glow discharge. J Appl Polym Sci 81(11):2769–2778
19. Chen X, Liu Z, Cao W et al (2015) Preparation, characterization, and antibacterial activities of quaternarized *N*-halamine-grafted cellulose fibers. J Appl Polym Sci. https://doi.org/10.1002/app.42702
20. Ma K, Liu Y, Xie Z et al (2013) Synthesis of novel *N*-halamine epoxide based on cyanuric acid and its application for antimicrobial finishing. Ind Eng Chem Res 52(22):7413–7418
21. Bastarrachea LJ, Goddard JM (2015) Antimicrobial coatings with dual cationic and *N*-halamine character: characterization and biocidal efficacy. J Agric Food Chem 63(16):4243–4251
22. Liu S, Sun G (2006) Durable and regenerable biocidal polymers: acyclic *N*-halamine cotton cellulose. Ind Eng Chem Res 45(19):6477–6482
23. Luo J, Porteous N, Lin J et al (2015) Acyclic *N*-halamine-immobilized polyurethane: preparation and antimicrobial and biofilm-controlling functions. J Bioact Compat Polym 30(2):157–166
24. Dong A, Zhang Q, Wang T et al (2010) Immobilization of cyclic *N*-halamine on polystyrene-functionalized silica nanoparticles: synthesis, characterization, and biocidal activity. J Phys Chem C 114(41):17298–17303
25. Thome J, Holländer A, Jaeger W et al (2003) Ultrathin antibacterial polyammonium coatings on polymer surfaces. Surf Coat Technol 174:584–587
26. Wang R, Xue H, Leng J et al (2022) Preparation and antibacterial properties of hemp cellulose-based material based on Schiff base between lysine grafted *N*-halamine and dialdehyde hemp[J]. Ind Crops Prod 176:114388
27. Wang F, Si Y, Yu J et al (2021) Tailoring nanonets-engineered superflexible nanofibrous aerogels with hierarchical cage-like architecture enables renewable antimicrobial air filtration. Adv Func Mater 31(49):2107223
28. Jiang L, Jia Z, Xu X et al (2022) Preparation of antimicrobial poly (ethylene-co-vinyl alcohol) membrane by grafting with *N*-halamine. React Funct Polym 172:105187
29. Islamipour Z, Zare EN, Salimi F et al (2022) Biodegradable antibacterial and antioxidant nanocomposite films based on dextrin for bioactive food packaging. J Nanostruct Chem 12:991
30. Aksakal B, Denktaş C, Bozdoğan A (2022) Influence of ultraviolet radiation on structural and uniaxial tensile characteristics of tannic acid/poly (vinyl alcohol) composite films. J Appl Polym Sci 139:52350
31. Fathi M, Rostami H, Youseftabar Miri N et al (2022) Development of an intelligent packaging by incorporating curcumin into pistachio green hull pectin/poly vinyl alcohol (PVA) films. J Food Meas Charact 16:1–10
32. Li R, Sheng J, Cheng X et al (2018) Biocidal poly (vinyl alcohol) films incorporated with *N*-halamine siloxane. Compos Commun 10:89–92
33. Zhou J, Zhang L, Shu H, Chen F (2002) Regenerated cellulose films from NaOH/urea aqueous solution by coagulating with sulfuric acid. J Macromol Sci Part B 41:1–15
34. Davoodi M, Kavoosi G, Shakeri R (2017) Preparation and characterization of potato starch-thymol dispersion and film as potential antioxidant and antibacterial materials. Int J Biol Macromol 104(Pt A):173–179

35. Tian H, Zhai Y, Xu C et al (2017) Durable antibacterial cotton fabrics containing stable acyclic *N*-halamine groups. Ind Eng Chem Res 56(28):7902–7909
36. Ali HE, Elbarbary AM, Abdel-Ghaffar AM et al (2022) Preparation and characterization of polyvinyl alcohol/polylactic acid/titanium dioxide nanocomposite films enhanced by γ-irradiation and its antibacterial activity. J Appl Polym Sci 24:52344
37. Mittal H, Kaith BS, Jindal R, Mishra SB, Mishra AK (2015) A comparative study on the effect of different reaction conditions on graft co-polymerization, swelling, and thermal properties of Gum ghatti-based hydrogels. Therm Anal Calorim 119(1):131–144
38. Li J, Liu Y, Jiang Z, Ma K, Ren X, Huang T-S (2014) Antimicrobial cellulose modified with nanotitania and cyclic *N*-halamine. Ind Eng Chem Res 53(33):13058–13064
39. Nawaz MA, Gaiani C, Fukai S, Bhandari B (2016) X-ray photoelectron spectroscopic analysis of rice kernels and flours: measurement of surface chemical composition. Food Chem 212:349–357
40. Demir B, Broughton RM, Huang TS, Bozack MJ, Worley SD (2017) Polymeric antimicrobial *N*-halamine-surface modification of stainless steel. Ind Eng Chem Res 56(41):11773–11781
41. Tang X, Xu H, Shi Y et al (2020) Porous antimicrobial starch particles containing *N*-halamine functional groups. Carbohyd Polym 229:115546
42. Idris C, Kocer Hasan B, Worley SD, Broughton RM, Huang TS (2011) *N*-halamine biocidal coatings via a layer-by-layer assembly technique. Langmuir 27(7):4091
43. Kocer Hasan B, Akin A, Worley SD, Orlando A, Broughton RM, Yonnie W (2010) Mechanism of photolytic decomposition of *N*-halamine antimicrobial siloxane coatings. ACS Appl Mater Interfaces 2(8):2456